Journal of Innovations in Engineering Education
JIEE 2025, Vol. 8, Issue 1.

https://doi.org/10.3126/jiee.v8i1.86583

THAPATHALI CAMPUS
Institute of Engineering
Tribhuvan University

Modeling bifacial PV performance under variable Albedo using Python: A case study of the Himalayan foothills, Kathmandu

Debendra Bahadur Raut[a,*], Bishal Kumar[a,b]

[a]*Department of Automobile and Mechanical Engineering, Thapathali Campus, Institute of Engineering, Tribhuvan University, Thapathali, Kathmandu, Nepal*

[b]*Department of Mechanical and Aerospace Engineering, Pulchowk Campus, Institute of Engineering, Tribhuvan University, Pulchowk, Lalitpur, Nepal*

ARTICLE INFO

Article history:

Received 18 November 2025
Revised in 25 December 2025
Accepted 29 December 2025

Keywords:

Bifacial PV
Bifacial radiance
Python
Albedo
Agrivoltaics
Ray-tracing
Specific yield

Abstract

The ground reflectance known as albedo has a significant impact on the performance of bifacial photovoltaic modules, which generate power from both their front and rear surfaces. Utilizing a Python-based workflow and NREL's bifacial radiance tool, this study aims to assess the energy yield of bifacial PV under variations in ground reflectance and albedo for the case of Kathmandu utilizing site-specific Typical Meteorological Year (TMY) data. An array of a 590 Wp bifacial module with a bifaciality factor of 0.80 is simulated at 4.0 m row pitch, 1.0 m clearance height, and 30° tilt. This study uses ray tracing simulations for a range of albedo values, from 0.18 to 0.75, taking temperature and loss correction factors into account. The findings show that bifacial gain increases almost linearly with albedo, from around 10% at 0.18 to 36% at 0.75. The results suggest that the performance of bifacial PV, particularly in agrivoltaic systems, can be significantly improved by reflecting ground cover and optimized array design. The Python-based approach offers a framework that may be modified for different locations and systems of a similar nature.

1. Introduction

By collecting sunlight on a module's front and rear surfaces, bifacial photovoltaic (PV) technology has the potential to significantly boost solar energy generation. In contrast to traditional monofacial systems, ground reflectance, or albedo, which varies based on surface type, vegetation, soil, and seasonal variations, has a significant impact on the extra energy from the back surface. Designing effective bifacial PV systems requires an understanding of how these parameters impact energy yield, especially in areas with high solar potential. The Himalayan foothills of Nepal offer perfect circumstances for evaluating bifacial PV performance because of their abundance of sunshine, mild temperatures, and varied agricultural landscapes.

Although bifacial PV performance has been examined worldwide, there is still a dearth of study on site-specific variables in Nepal. Specifically, no previous work has combined realistic albedo situations, high-resolution ray-tracing simulations, and local weather data for the Kathmandu region. Additionally, a lot of current evaluations make the assumption that albedo values are fixed, which leaves out the seasonal variability that is characteristic of solar PV systems.

Optimizing system design and ground management methods requires an understanding of how albedo affects bifacial PV output in Nepal's ground-mounted and agrivoltaic systems. This study offers precise, transparent, and flexible simulations that can be applied to different locations and system configurations through the use of a repeatable Python-based bifacial radiance modelling workflow. By simulating energy yields across a range of albedo values representing various ground conditions, comparing the results with monofacial systems to quantify bifacial gain, and developing a repeatable Python-based modelling framework that can be applied to future site-specific studies, this study seeks to assess bifacial PV performance in Kathmandu. Instead

*Corresponding author:
raut.debendra@tcioe.edu.np (D.B. Raut)

of using direct on-site performance measurements, the study is based on simulations employing TMY/EPW data. Furthermore, the analysis only looks at a small, representative PV array; future research will need to evaluate the effects of scaling up to larger installations. Because they may produce more energy than traditional monofacial systems, bifacial photovoltaic (PV) systems are gaining popularity. However, because of the complex interactions of light on and around the modules, modelling their energy yields is more difficult.

This review of the literature compiles previous research on the impact of albedo on bifacial PV specific yield, emphasizes comparisons with monofacial modules, and looks at popular simulation tools like bifacial_radiance, PVsyst, and SAM, which are frequently used to model the performance of bifacial systems.

The percentage of incident solar radiation that a surface reflects, or albedo, varies greatly. For example, fresh snow may reflect 55–98% of sunlight, but darker soils may reflect 8–23%. Bifacial gain, which is the percentage increase in energy yield over a similar monofacial system, is frequently used to describe the performance of bifacial PV systems. Accurate modelling of albedo effects is crucial because sites with higher albedo might produce noticeably bigger bifacial advantages. Increased albedo, more diffuse sunlight, taller module mounting, and wider row spacing are generally associated with increased bifacial gain [1].

Bifacial PV performance is significantly influenced by albedo levels, which vary based on the kind of surface. The albedo of grass, which is frequently utilized in field or agrivoltaic installations, ranges from 0.15 to 0.26, with temperate climes typically using 0.18 [2]. One of the most common surfaces for ground-mounted PV systems is soil or natural ground, which typically ranges from 0.1 to 0.3, with 0.2 commonly employed in simulations [3]. Albedo values for concrete rooftops, which are common in urban flat-roof installations, range from 0.30 to 0.35, with 0.32 being selected for modelling [4]. Dry sand, which is frequently found in desert-like settings, reflects between 30 and 40 percent of sunlight; in Middle Eastern models, 0.35 is a typical value [5]. Snow has the maximum reflectivity, ranging from 0.7 to 0.85; Canadian-based studies often use 0.75 [6].

Actual daylight albedo varied between 0.15 and 0.22, according to a research conducted on a rooftop in Beijing. Using a fixed value of 0.20 resulted in a 19.4% overestimation of rear-side irradiation [7]. Similarly, if sky-view effects are not taken into account, theoretical calculations show that assuming shaded ground is evenly reflective can overstate energy output by 5-9% [8]. In order to solve these problems, contemporary modelling programs frequently let users select between fixed and variable albedo options, allowing inputs like spectral albedo models, hourly readings, or even a constant albedo [9][10]. The anticipated bifacial PV performance may be significantly impacted by these decisions.

Bifacial PV is the special focus of a number of new Python-based solutions. Notably, bifacial_radiance can simulate annual irradiance on intricate 3D array landscapes and offers a high-resolution ray-tracing framework for front and rear irradiance that include interactions with the ground and adjacent structures [11][12][13]. Although there are other Python tools like BifacialSimu, pvfactors (view-factor based), and some commercial software like PVsyst and SAM, academic research is increasingly favoring open Python code due to its adaptability, customization, and reproducibility.

Bifacial benefits ranged from as little as 2.5% in low-albedo southern regions to up to 22% in the Himalayas, where greater albedo and taller mounting structures contributed to improved production, according to a simulation conducted throughout India [14]. A Brazilian plant obtained a 6.2% gain at a soil albedo of 0.11 when front and rear sides were examined independently [15], while rooftop experiments in Bangladesh revealed 10-15% more energy depending on module tilt and orientation [12]. These results demonstrate how crucial site-specific albedo is for precise performance forecasting. As a result, comprehensive modelling is required, and tools like bifacial_radiance and BifacialSimu, which are being used more and more to describe albedo effects in a variety of climates, are still being improved [9][13].

For bifacial systems, raising albedo from 0.2 to 0.3 can result in an annual energy output increase of up to 5%, according to simulations using PVsyst [16]. The significance of module clearance height was highlighted by radiance-based studies investigating the spectrum influence of crop albedo (0.18-0.25), which found an 8-12% energy uplift for elevated arrays (1-2 m clearance) compared to ground-mounted systems [17][18]. In actual installations like those in Chile and California, field data from the IEA PVPS study show bifacial gains of 5–12% at albedo values between 0.2 and 0.3 [19]. At an albedo of 0.25, ground-mounted bifacial systems usually show benefits of less than 10%, increasing to about 30% when albedo hits 0.5 and modules are raised one meter from the ground [20]. Bifacial gains exceeded 20% for reflective surfaces including concrete, white tile, and white pebbles, compared to 5–10% for soil, according to comparative tests conducted at Heriot-Watt University (UK) [4]. These patterns are further sup-

ported by real-world validation using Soltec's BiTEC data in California, which reveals gains of 15.7% at high albedo (0.56) and 9.6% at intermediate albedo (0.295) [21]. Seasonal differences were also noted in a 2024 modelling study published in EPJ PV, with bifacial gains of 9.8–11.7% in spring, summer, and autumn and a peak of 28.4% in winter as a result of snow-induced albedo enhancements [22].

Although research from around the world emphasizes the significance of ground albedo and diffuse irradiance for bifacial gains, Nepal's particular combination of high altitude and monsoon-influenced climate results in significant seasonal variations in soil reflectance, vegetation cover, and aerosol levels—factors that have been mostly ignored. Standard models and fixed-albedo assumptions are unable to account for the considerable variations in rear-side irradiance that can result from these dynamic situations.

Although there are currently few comprehensive performance evaluations from Nepal, bifacial PV systems are beginning to be used commercially in Kathmandu and other locations. Despite the lack of formal field tests, mono-PERC bifacial modules for rooftop and small ground-mounted projects are now offered by a number of local EPC companies and distributors, indicating that the technology has started to enter the domestic market. This early acceptance emphasizes the necessity of the current simulation work, which aids in estimating potential bifacial gains in Kathmandu's conditions prior to the development of larger projects. The increasing number of these modules suggests that the technology is already being deployed in practice, even though no location in Kathmandu has yet to produce measurable bifacial performance data.

In order to close this gap, this work simulates bifacial PV performance in Kathmandu under realistic conditions using NREL's verified bifacial_radiance ray-tracing tool. It offers the first high-resolution, climate-sensitive evaluation of bifacial PV customized for Nepal by taking into account seasonal albedo variations, aerosol effects, and local meteorological data. This creates a framework for future PV system planning, including agrivoltaic installations in challenging terrain.

2. Research Methodology

Bifacial PV performance can be estimated using a variety of modelling techniques, which vary in terms of accuracy, computational effort, complexity, and necessary inputs. View-factor techniques are used by analytical models, such the PVlib-Python framework, to determine front and rear irradiance depending on the area of the sky and ground that the module can see. These models are quick and easy to compute, but they are unable to capture reflections from surrounding objects or intricate 3D shading [23][24].

On the other hand, numerical models such as bifacial_radiance use ray-tracing techniques to simulate the actual 3D behavior of light. Based on the Radiance engine, bifacial_radiance can accurately calculate irradiance on both module surfaces, account for sky and sun locations using the Perez sky model, and depict realistic PV system designs [25]. It provides a physically detailed estimate of energy yield by using a backward ray-tracing method to record shadows, reflections, and light diffusion in a virtual scenario that incorporates real weather data, geography, and system configuration [26].

For these reasons, this study employs the bifacial_radiance approach. The methodology is structured into five phases: (1) Data acquisition (site and meteorological inputs), (2) PV module and array configuration, (3) Sky model and scene generation, (4) Radiance ray-tracing analysis, and (5) Energy yield calculation. Each phase is described below, including relevant equations and computational steps.

A flowchart for the bifacial PV performance simulation is shown in Figure 1. The site location, PV module specs, array layout, and environmental information like albedo and weather are among the inputs. The procedures include analyzing meteorological data, building a sky model and 3D array scene using Radiance, calculating module irradiance using ray-tracing analysis, and then calculating PV power. A complete image of the system's performance is provided by the outputs, which include energy yield metrics, effective irradiance values, and front and rear irradiance maps.

2.1. Site and meteorological data

A Typical Meteorological Year (TMY) EPW file with location-specific meteorological data for Kathmandu (latitude 27.7°, longitude 85.3°) is used in the simulation to provide hourly values of GHI, DNI, DHI, air temperature, wind speed, and other pertinent inputs. The Radiance gendaylit tool reconstructs the sky luminance distribution for both direct and diffuse irradiance using these data for sky modelling [26]. The sun position, associated irradiance, and ambient conditions are calculated by PVLib routines for each daylight hour (6:00–18:00) after meteorological inputs are read into a MetObj. To maximize calculation, all times are localized to the site's time zone.

2.2. PV module and array configuration

The physical and electrical properties of the bifacial PV module define it. This work models a 590 Wp bi-

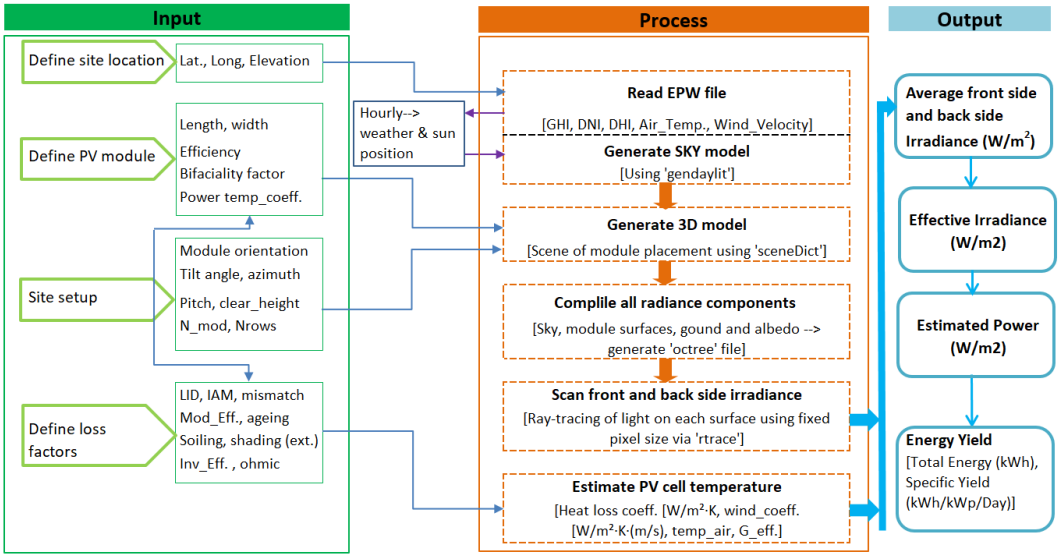

Figure 1: Methodological approach of the simulation model

facial module (length 2.278 m, width 1.134 m) with a front-side efficiency of 22.84% at STC and a bifaciality factor of 0.8, which indicates that the rear side contributes 80% as effectively as the front. A 30° tilt, a south-facing azimuth (180°), a row pitch of 4.0 m, a clearance height of 1.0 m, two modules per row, and a total of two rows comprise the array arrangement. In order to account for system inefficiencies, fixed loss factors such as light-induced degradation (2%), mismatch (1%), module degradation (0.8%), angle of incidence losses (2.5%), Ohmic losses (1%), soiling (3%), inverter conversion (2%), shading (1.2%), and ageing (0.5%) are applied after the PVsyst loss budget.

2.3. Sky model and scene generation

Radiance's gendaylit application is used via radiance_obj.gendaylit to create a sky description for every simulated hour. While PVLib determines the sun's position (zenith, altitude, and azimuth) using time, date, and site coordinates, this procedure enters the timestamp and meteorological data. Gendaylit then computes the sky radiance distribution from the measured DNI and DHI to build a fisheye sky representation using the Perez all-weather sky model. The result is a Radiance sky file that shows the real sky conditions for that hour, including the sun disc and sky dome [26].

Radiance_obj.makeScene(module, sceneDict), which creates a SceneObj with the array geometry, is used to create the 3D PV array scene. The tilt, azimuth, row pitch, number of modules and rows, and mounting height are all specified by the sceneDict. Each row of modules in this fixed-tilt array is positioned in accordance with the specified pitch and clearance height [27]. Radiance_obj.setGround(alb) is used to depict the ground as an infinite plane with uniform albedo, rendered as a Lambertian surface to account for diffuse reflection [28]. Lastly, radiance_obj.makeOct() creates an octree file, a spatial structure that facilitates effective ray-tracing of irradiance and radiance in Radiance, by combining the modules, ground, and sky.

2.4. Radiance ray-tracing analysis

The methodology relies heavily on ray-tracing simulation to calculate irradiance on module surfaces. Using AnalysisObj.moduleAnalysis(scene, sensorsy, sensorsx), scan points (sensors) are first defined on the modules, where sensorsy and sensorsx form a grid across the width and length of the module [29]. For irradiance sampling, the frontscan and backscan dictionaries capture one point that is marginally above and below the module centre (offset by 0.001 m).

Ray tracing is then performed via analysis.analysis(octfile, name, frontscan, backscan). Using backward ray tracing, Radiance traces rays from each sensor into the 3D scene to integrate contributions from the sky and ground, effectively solving the rendering equation for irradiance (as shown in Equation 1).

$$E = \int L_{\text{sky}}(\omega)\cos\theta\, d\omega + \int L_{\text{ground}}(\omega)\cos\theta\, d\omega \quad (1)$$

In this equation, L_{sky} and L_{ground} represent the radi-

ance from the sky and ground along direction ω, while $\cos\theta$ accounts for the angle between ω and the module surface normal. Radiance performs this integration by sampling sky patches and the sun [25]. Shading, reflections, and diffuse sky contributions are captured by the output, which is the irradiance (W/m^2) at each sensor for both front and back surfaces. In practice, the total module irradiance is represented by averaging the sensor measurements.

2.5. Effective irradiance

The effective irradiance on a bifacial module is calculated as shown in Equation 2:

$$G_{\text{eff}} = G_f + \beta_m G_r \tag{2}$$

where G_f and G_r are the front and rear irradiances, and β_m is the module's bifaciality factor. This formulation reflects the fact that rear-side irradiance contributes at reduced efficiency. For instance, with $\beta_m = 0.8$ in this study, 80% of the rear irradiance is considered equivalent to front-side irradiance [25].

2.6. Estimation of PV cell temperature and coefficient of losses

The PV cell temperature (T_cell) is estimated using the empirical heat-loss model from PVsyst [25]. The cell temperature rises above ambient due to absorbed irradiance and is calculated as shown in Equation 3:

$$T_{\text{cell}} = T_a + \frac{\alpha_a G_{\text{eff}} (1 - \eta)}{U_c + U_v V} \tag{3}$$

where T_a is the ambient temperature, G_{eff} is the effective irradiance (W/m^2), V is the wind speed (m/s), $\alpha_a \approx 0.9$ is the absorption coefficient, η is the electrical efficiency, $U_c \approx 29\ W/m^2K$ is the heat-loss coefficient, and $U_v \approx 1\ W/m^2K{\cdot}m/s$ is the wind-dependent coefficient for free-standing modules. In this study, the code simplifies $\alpha_a G_{\text{eff}} (1-\eta)$ to unity, consistent with PVsyst [25].

The temperature-corrected module efficiency is then applied using the module's temperature coefficient $\gamma = -0.29\%/°C$ as shown in Equation 4:

$$\eta_{T_{\text{cell}}} = 1 + \gamma (T_{\text{cell}} - 25\,°C) \tag{4}$$

The overall module efficiency accounting for temperature and other fixed losses is given as shown in Equation 5.

$$\eta_{\text{total}} = \eta_{\text{STC}} \cdot \text{CoL} \tag{5}$$

where CoL is the combined coefficient of losses, incorporating $\eta_{T_{\text{cell}}}$ and $\eta_{\text{fixed losses}}$.

The power density is then calculated as shown in Equation 6.

$$P_{\text{dens}} = \eta_{\text{total}} G_{\text{eff}} \tag{6}$$

The total array power output at the inverter for each hour is calculated using Equation 7.

$$P_{\text{out}} = P_{\text{dens}} N_{\text{mods}} N_{\text{rows}} A_{\text{module}} \tag{7}$$

where N_{mods} and N_{rows} are the number of modules per row and the number of rows, respectively, and A_{module} is the module area. The code converts this to kW, integrates over each hour to obtain kWh, and sums hourly values to calculate monthly and annual energy outputs. Monthly averages of irradiance and power are computed by averaging daily values, and the annual specific yield (kWh/kWp per year) is determined by dividing total annual energy by the system's nameplate capacity [30].

3. Results and discussion

The daily average values of DHI (diffuse horizontal irradiance, sunlight diffused by the sky), DNI (direct normal irradiance, sunlight coming straight from the sun), and GHI (global horizontal irradiance, total sunshine on a horizontal surface) are shown in Figure 2. The sky model, front and back module irradiance calculations, and seasonal PV performance analysis all depend on these irradiance components.

The curves in Figure 3 represent daily energy values, with GHI at 5.08, DNI at 4.37, and DHI at 2.27 $kWh/m^2/day$.

Table 1 presents the monthly averages of GHI, DNI, DHI, temperature, and wind speed for 2021 used in the simulations. The average daily GHI is approximately 5.08 $kWh/m^2/day$, with higher values in spring and lower values during the monsoon, establishing the baseline solar resource for the study.

As ground albedo changed, the simulation examined energy yields for bifacial and monofacial PV systems. Bifacial modules are extremely sensitive to ground reflectance, in contrast to monofacial modules, which only record front-side irradiance. Both system yields increased with increasing albedo, but the bifacial yield increased significantly more quickly. Bifacial increase, for instance, was 15.8% at 0.30, 20.5% at 0.40, and 36% at 0.75. Monofacial yields, on the other hand, only marginally increased roughly 0.6–2.2% for 0.1 albedo increment because higher reflectance only significantly

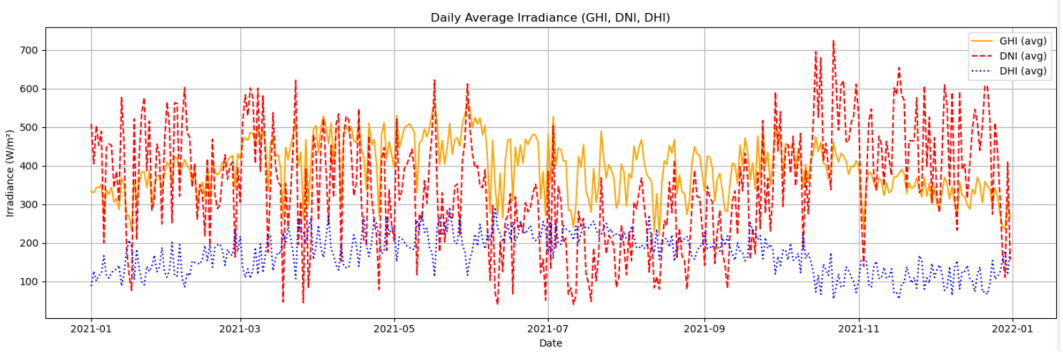

Figure 2: Solar radiance data on the site for year 2021 (TIA station, NPL, SWERA, 444540, 27.70, 85.37, 5.75, 1337.0)

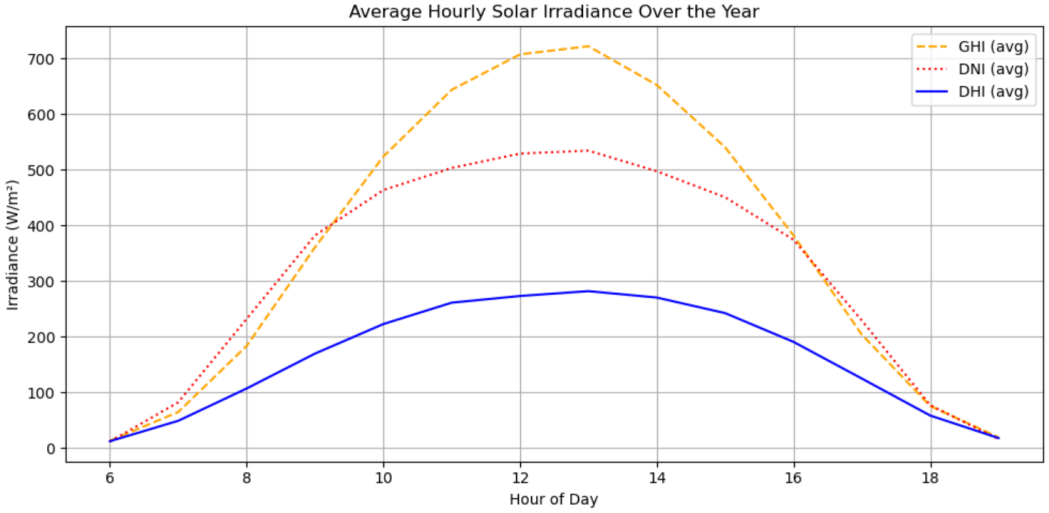

Figure 3: Yearly average radiation data from 6am to 6pm

increases the amount of diffuse light that reaches the front side. According to these findings, bifacial modules perform better than monofacial ones under the same sky conditions because higher ground reflectance considerably increases the rear-side contribution.

Table 2 summarizes the key quantitative results for specific yield and bifacial gain at each albedo level, providing a basis for analyzing trends and comparing with previous studies.

In summary, the analysis shows that one important element affecting bifacial PV performance is ground albedo. The rear-side contribution is greatly increased by higher albedo, which enables bifacial modules to produce significantly more energy than monofacial systems.

The specific yield of monofacial and bifacial PV systems was analyzed for varying ground albedo values (as shown in Figure 4). Monofacial performance showed only a weak dependence on albedo, following the fitted relationship as shown in Equation 8.

$$Y_{\text{mono}} = 0.28\,\alpha + 4.49 \quad (R^2 = 0.9990) \tag{8}$$

where α is the albedo and Y_{mono} is the specific yield in kWh/kWp/day. Each 0.10 increase in albedo corresponded to a modest 0.0286 kWh/kWp/day rise (0.6% from baseline).

Bifacial systems exhibited a much stronger dependence, as shown in Equation 9.

$$Y_{\text{bi}} = 2.45\,\alpha + 4.57 \quad (R^2 = 0.9999) \tag{9}$$

Here, a 0.10 increase in albedo resulted in 0.2455 kWh/kWp/day (4–5% increase).

The bifacial gain, defined as the percentage increase over the monofacial yield, is given by Equation 10.

$$G_{bi} = 45.40\,\alpha + 2.17 \quad (R^2 = 0.9996) \qquad (10)$$

This corresponds to a gain increase of 4.54% per 0.10 albedo increment, with simulated gains ranging from 10% at $\alpha = 0.18$ to 36% at $\alpha = 0.75$, consistent with the regression results.

The bifacial gain fitted model closely matches empirical findings from Soltec's BiTEC study, which found gains of 7.3%, 9.6%, and 15.7% for albedos of around 0.20, 0.30, and 0.55, respectively [31]. The model's validity within the practical albedo range of 0.18–0.75 is supported by this agreement. In general, bifacial gains of 5–30% are reported in the literature; when albedo is 0.50 and module elevation is optimised, values can reach approximately 30% [22][20]. The array component of DHI as opposed to GHI, geometry, including mounting height, row spacing (GCR), tilt, and mutual shading effects, can all be blamed for minor differences in the results.

Bifacial energy gains are typically between 5% and 30%, depending on a variety of criteria (albedo, installation height, ground covering, geographic location, etc.), according to data collected (global field data) and models. The following average range of energy gain has been validated by regional field studies: When comparing the computed energy gain by bifacial installations with the corresponding values of local albedo, the study conducted in India by Johnson & Manikandan (2023) reveals that the maximum energy gain resulting from variations in local albedo, soil albedo, and installation height is between 2.5% and 25%. These findings are in good agreement with the results presented in this study. Bifacial energy gain ranges from 22.6% to 25% for albedo values between 0.36 and 0.4 [14].

A field study in Minas Gerais reported an additional 6.2% energy yield at a soil albedo of 0.11. This relatively low gain is consistent with our simulation, which predicts an approximate 10% increase at $\alpha = 0.18$, after accounting for differences in module height and latitude [15].

The discrepancies between measured and simulated bifacial performance have not been extensively studied. These discrepancies typically result from variations in albedo, shading, soiling, spectral effects, and ground

Table 1: Yearly summary of weather file

Date [YY-MM]	Avg. GHI (W/m²)	Avg. DNI (W/m²)	Avg. DHI (W/m²)	Avg. Temp (°C)	Avg. Wind (m/s)
2021-01	335.44	396.03	132.66	12.73	1.27
2021-02	383.20	381.75	158.89	14.26	1.42
2021-03	435.00	379.46	181.95	18.03	1.80
2021-04	454.20	356.29	196.01	21.52	2.12
2021-05	479.50	355.33	210.69	22.93	1.73
2021-06	420.16	250.79	224.50	24.40	1.79
2021-07	375.81	195.72	225.46	24.48	0.88
2021-08	376.51	233.40	198.62	24.04	1.07
2021-09	391.66	287.32	190.74	23.29	1.20
2021-10	417.01	475.22	132.22	21.94	1.15
2021-11	349.26	446.29	114.01	16.26	0.85
2021-12	316.74	415.09	115.92	13.46	1.15
Average	394.54	347.72	173.47	19.78	1.37

Table 2: Specific yield (kWh/kWp/day) and bifacial gain (%) for different ground albedo values (annualized)

Albedo	Specific Yield (kWh/kWp/day)		Bifacial Gain (%)
	Monofacial	Bifacial	
0.18	4.55	5.01	10.1
0.20	4.55	5.06	11.1
0.30	4.58	5.31	15.8
0.40	4.61	5.56	20.5
0.75	4.71	6.41	36.0

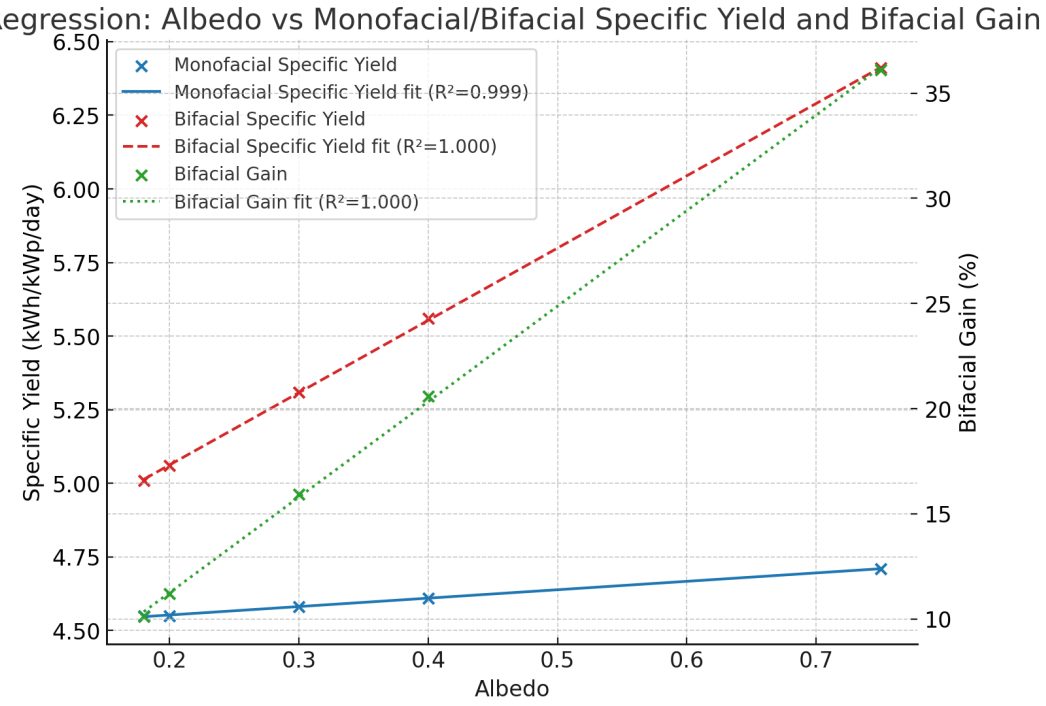

Figure 4: Fitting of specific yield and bifacial gain as function of albedo values

conditions that are hard to replicate in models. Beijing rooftop study (Su et al., 2024): Because daytime albedo varied between 0.15 and 0.22, using a fixed albedo of 0.20 resulted in a 19.4% overestimation of rear-side irradiance compared to observations. This demonstrates how simulations are sensitive to real-world ground and roof reflectance [7].

Recent research has used real data from utility scale and demonstration plants in Golden, USA; Heggelbach, Germany; and Florianopolis, Brazil, to validate the open-source BifacialSimu framework. When compared to measured outputs, the annual energy yield predicted by BifacialSimu across these sites typically showed relative errors within ±5 to 15%. Configurations that combined precise site-specific inputs like albedo, mounting height, and row spacing with detailed ray tracing yielded the lowest deviations. The significance of 3D effects and realistic treatment of rear side irradiance in bifacial performance modelling is highlighted by the fact that hybrid or complete ray tracing modes generally produced smaller bias and lower normalized Root Mean Square Error (RMSE) than pure view factor techniques [32].

In this work, field measurements at two locations (fixed tilt in Albuquerque, NM and single axis tracker in Davis, CA) were used to benchmark four bifacial irradiance models: bifacial_radiance (ray tracing), bifacialvf, pvfactors, and PVsyst. The simpler view factor models matched the accuracy of the more computationally costly ray tracing strategy, and all models projected annual bifacial gain within around ±1% of one another [33].

In order to determine how sensitive bifacial gain is to configuration, a number of rear irradiance models for bifacial PV were tested across a variety of design parameters (clearance height, row spacing, tilt, and albedo). According to the paper, bifacial increases of up to 20% are achievable in some configurations. At low ground clearances, different models agree well, but diverge significantly when modules are mounted higher, where edge effects and finite array size become significant. Higher clearances result in more uniform rear side irradiation, and when compared to measurements from a test bed in Golden, Colorado, bifacial gain estimations from the models generally match with field data within about 2 percentage points for appropriate designs [34].

These investigations unequivocally demonstrate that although ray-tracing methods like bifacial_radiance generate dependable patterns and relative trends, dynamic, site-specific variables might result in significantly worse field performance. This demonstrates why local validation is necessary in areas like Kathmandu.

4. Conclusion

In order to assess the effect of different ground albedo on bifacial PV performance in the Himalayan foothills of Kathmandu, this study employed a repeatable, Python-based bifacial_radiance process. Bifacial gain increased almost linearly with albedo, from approximately 10% at low reflectance ($\alpha = 0.18$) to approximately 36% at high reflectance ($\alpha = 0.75$), according to the models. These findings demonstrate that surface treatment and array geometry are important design elements for maximizing the energy yield of bifacial PV systems. The methodology offers useful insights for PV developers, agrivoltaic practitioners, and policymakers seeking integrated approaches to food and energy production by combining site-specific meteorological data with comprehensive ray-tracing. Additionally, the Python procedure ensures complete reproducibility and is adaptable to different locations, system configurations, and seasonal ground conditions.

In order to enable direct validation of the modelled albedo fluctuations and a more thorough comparison between simulation-based forecasts and field-based performance data, future work will expand this simulation framework with on-site measurements from bifacial PV arrays in Kathmandu.

Acknowledgement

The authors affirm that the work described in this publication was not influenced by any known competing financial interests or personal relationships.

References

[1] International Energy Agency (IEA) PVPS. Bifacial photovoltaic modules and systems: Experience and results from international research and pilot applications (iea-pvps t13-14:2021)[R]. International Energy Agency Photovoltaic Power Systems Programme, 2021.

[2] Pelaez S A, Deline C, Greenberg P, et al. Model and validation of single-axis tracking with bifacial pv[J/OL]. IEEE Journal of Photovoltaics, 2019, 9(3): 715-721. DOI: 10.1109/JPHOTOV.2019.2892872.

[3] International Energy Agency Photovoltaic Power Systems Programme. Best practices for the optimization of bifacial photovoltaic tracking systems (iea-pvps t13-26:2024)[R/OL]. IEA, 2024. DOI: 10.69766/JOIK1919.

[4] Alam M, Gul M S, Muneer T. Performance analysis and comparison between bifacial and monofacial solar photovoltaic at various ground albedo conditions[J/OL]. Renewable Energy Focus, 2023, 44: 295-316. DOI: 10.1016/j.ref.2023.01.005.

[5] Zhang X, Jiao Z, Zhao C, et al. Review of land surface albedo: Variance characteristics, climate effect and management strategy[J/OL]. Remote Sensing, 2022, 14(6): 1382. DOI: 10.3390/rs14061382.

[6] Appelbaum J. Bifacial photovoltaic panels field[J/OL]. Renewable Energy, 2016, 85: 338-343. DOI: 10.1016/j.renene.2015.06.050.

[7] Su X, Luo C, Chen X, et al. Numerical modeling of all-day albedo variation for bifacial pv systems on rooftops and annual yield prediction in beijing[J]. Building Simulation, 2024, 17: 955-964.

[8] d'Alessandro V, Daliento S, Dhimish M, et al. Albedo reflection modeling in bifacial photovoltaic modules[J]. Solar, 2024, 4(4): 660-673.

[9] Grommes E M, Schemann F, Klag F, et al. Simulation of the irradiance and yield calculation of bifacial pv systems in the usa and germany by combining ray tracing and view factor model[J]. EPJ Photovoltaics, 2023, 14.

[10] Grommes E M, Blieske U. Bifacialsimu: Holistic simulation of large-scale bifacial photovoltaic systems[J]. Journal of Open Source Software, 2022, 7(78): 4443.

[11] Bifacial_radiance training: Part 1[EB/OL]. DOI: https://docs.nrel.gov/docs/fy20osti/75218.pdf.

[12] Catching rays: How bifacial_radiance sheds light on the future of solar pv[EB/OL]. https://docs.nrel.gov/docs/fy24osti/91122.pdf.

[13] (NREL) N R E L. Photovoltaic bifacial irradiance and performance modeling toolkit[EB/OL]. 2025. https://www.nrel.gov/pv/pv-bifacial-irradiance-toolkit.

[14] Johnson J, Manikandan S. Resource potential mapping of bifacial photovoltaic systems in india[J]. iScience, 2023, 26(10).

[15] Braga D S, Kazmerski L L, Cassini D A, et al. Performance of bifacial pv modules under different operating conditions in the state of minas gerais, brazil[J/OL]. Renewable Energy Environ. Sustain., 2023, 8. DOI: 10.1051/rees/2023025.

[16] Khan I, Pathak M J M, Tripathi A. Vertical bifacial solar farms: Physics, design, and global optimization[J/OL]. Applied Energy, 2021, 206: 240-248. DOI: 10.48550/arXiv.1812.07849.

[17] Marrou H. Productivity and radiation use efficiency of lettuces grown in the partial shade of photovoltaic panels[J/OL]. European Journal of Agronomy, 2013, 44: 54-66. DOI: 10.1016/j.eja.2012.08.003.

[18] Amaducci S, Yin X, Colauzzi M. Agrivoltaic systems to optimise land use for electric energy production[J/OL]. Applied Energy, 2018, 220: 545-561. DOI: 10.1016/j.apenergy.2018.03.081.

[19] IEA-PVPS Task 13. Bifacial photovoltaic modules and systems: A review of pvps task 13 performance and reliability findings (report no. iea-pvps t13-14:2021)[R/OL]. International Energy Agency Photovoltaic Power Systems Programme, 2021. https://iea-pvps.org/wp-content/uploads/2021/04/IEA-PVPS-T13-14_2021-Bifacial-Photovoltaic-Modules-and-Systems-report.pdf.

[20] Sun X, Khan M R, Deline C, et al. Optimization and performance of bifacial solar modules: A global perspective[J/OL]. Applied Energy, 2018, 212: 1601-1610. DOI: 10.1016/j.apenergy.2017.12.041.

[21] Soltec. The bifacial year: Bitec annual results on bifacial gain under different albedo conditions[EB/OL]. 2019. https://www.soltec.com/uploads/2019/11/BiTEC-whitepaper-4_en.pdf.

[22] Ghafiri S, Darnon M, Davigny A, et al. A comprehensive performance evaluation of bifacial photovoltaic modules: Insights from a year-long experimental study conducted in the canadian climate[J/OL]. EPJ Photovoltaics, 2024, 15. DOI: 10.1051/epjpv/2024025.

[23] pvlib-python Development Team. pvlib.bifacial.pvfactors.pvfactors_timeseries - pvlib python 0.13.1 documentation[EB/OL]. 2024. https://pvlib-python.readthedocs.io/en/latest/reference/generated/pvlib.bifacial.pvfactors.pvfactors_timeseries.html.

[24] pvlib-python Development Team. pvlib.bifacial.infinite_sheds.get_irradiance - pvlib python 0.13.1 documentation[EB/OL]. 2024. https://pvlib-python.readthedocs.io/en/latest/reference/generated/

pvlib.bifacial.infinite_sheds.get_irradiance.html.
[25] Pelaez S A, Deline C. Bifacial_radiance training: Part 1 (nrel/pr-5k00-75218)[R/OL]. National Renewable Energy Laboratory, 2019. https://docs.nrel.gov/docs/fy20osti/75218.pdf.
[26] Ward G J. Gendaylit: A program to generate a sky description for daylight simulation[EB/OL]. https://www.radiance-online.org/learning/documentation/manual-pages/pdfs/gendaylit.pdf.
[27] bifacial_radiance developers. Radianceobj.makescene - bifacial_radiance 0.4.5.dev1+g8c76450 documentation[EB/OL]. . https://bifacial-radiance.readthedocs.io/en/latest/generated/bifacial_radiance.RadianceObj.makeScene.html.
[28] bifacial_radiance developers. Radianceobj.gendaylit - bifacial_radiance documentation[EB/OL]. . https://bifacial-radiance.readthedocs.io/en/latest/generated/bifacial_radiance.RadianceObj.gendaylit.html.
[29] bifacial_radiance developers. Analysisobj.moduleanalysis - bifacial_radiance documentation[EB/OL]. . https://bifacial-radiance.readthedocs.io/en/latest/generated/bifacial_radiance.AnalysisObj.moduleAnalysis.html.
[30] PVsyst SA. Array thermal losses[EB/OL]. https://www.pvsyst.com/help/project-design/array-and-system-losses/array-thermal-losses/index.html.
[31] Soltec. The bifacial year[EB/OL]. 2023. https://soltec.com/en/innovation/lab/the-bifacial-year/.
[32] Grommes E M, Koch M, Hadji-Minaglou J R, et al. Towards precision in bifacial photovoltaic system simulation: a model selection approach with validation[J/OL]. Frontiers in Energy Research, 2025, 13. DOI: 10.3389/fenrg.2025.152768.
[33] Asgharzadeh A. A benchmark and validation of bifacial pv irradiance models[C/OL]// 2019 IEEE 46th Photovoltaic Specialists Conference (PVSC). 2019: 3281-3287. DOI: 10.1109/PVSC40753.2019.8981272.
[34] Pelaez S A, Deline C, MacAlpine S M, et al. Comparison of bifacial solar irradiance model predictions with field validation[J/OL]. IEEE Journal of Photovoltaics, 2019, 9(1): 82-88. DOI: 10.1109/JPHOTOV.2018.2877000.